

Methods

Molecular dynamics (MD) calculations are performed for 512 molecules contained in a cubic box with the periodic boundary. A time step in MD is 1 fs (femtosecond; 10^{-15} s). In the present study, a constant-volume (0.96 g cm^{-3}) and constant-temperature MD is employed. The Nose–Hoover method is used to control the temperature. An empirical water model, TIP4P, is used to describe the water–water molecular interaction. Intermolecular interaction is cut off smoothly as in previous studies^{5,6,16}. MD trajectories are performed for different temperatures, but so far only one at 230 K undergoes the crystallization for 512 water molecules. We have performed 6 trajectory calculations of the order of microseconds, but only the one that successfully crystallized is presented in this work. An individual trajectory calculation of this size system takes several months in a supercomputer. One trajectory with 220 K is found to stop in a partially crystallized structure. Those with higher temperatures have never resulted in freezing. MD calculations were also performed for various size systems containing 64, 96, 216, and 4,096 water molecules. For 4,096 water molecules, a freezing process is also attained at 230 K. Constant-pressure and constant-temperature trajectories have also been performed for various sizes of systems but crystallization has so far been achieved only for a very small system (64 water molecules). These constant-pressure, constant-temperature trajectories show that large density fluctuations are always associated with the freezing process. An inherent structure analysis²⁶ is performed by applying a local quenching method; the inherent structures are local minima of the potential wells sequentially visited by the system in a trajectory. In the inherent structure description, vibrational motions are thus removed, revealing the fundamental hydrogen-bond structure changes along the trajectory^{4–6,26}.

Received 22 December 2001; accepted 19 February 2002.

1. Swope, W. C. & Andersen, H. C. 10^6 particle molecular-dynamics study of homogeneous nucleation of crystals in a supercooled atomic liquid. *Phys. Rev. B* **41**, 7042–7054 (1990).
2. Wolde, P. R. & Frenkel, D. Enhancement of protein crystal nucleation by critical density fluctuation. *Science* **277**, 1975–1978 (1997).
3. Ball, K. D. *et al.* From topographies to dynamics on multidimensional potential energy surfaces of atomic clusters. *Science* **271**, 963–966 (1996).
4. Ohmine, I. & Saito, S. Water dynamics: fluctuation, relaxation, and chemical reactions in hydrogen bond network rearrangement. *Acc. Chem. Res.* **32**, 741–749 (1999).
5. Ohmine, I. Liquid water dynamics; collective motions, fluctuation and relaxation. *J. Phys. Chem.* **99**, 6767–6776 (1995).
6. Ohmine, I. & Tanaka, H. Fluctuation, relaxation and hydration in liquid water. Hydrogen-bond rearrangement dynamics. *Chem. Rev.* **93**, 2545–2566 (1993).
7. Svishchev, I. M. & Kusalik, P. G. Electrofreezing of liquid water: A microscopic perspective. *J. Am. Chem. Soc.* **118**, 649–654 (1996).
8. Nada, N. & Furukawa, Y. Anisotropic growth kinetics of ice crystals from water studied by molecular dynamics simulation. *J. Cryst. Growth* **169**, 587–597 (1996).
9. Koga, K., Tanaka, H. & Zeng, X. C. First-order transition in confined water between high-density liquid and low-density amorphous phases. *Nature* **408**, 564–567 (2000).
10. Onuchic, J. N., Luthey-Schulten, Z. & Wolynes, P. G. Theory of protein folding: the energy landscape perspective. *Annu. Rev. Phys. Chem.* **48**, 545–600 (1997).
11. Dobson, C. M. & Karplus, M. The fundamentals of protein folding: bringing together theory and experiment. *Curr. Opin. Struct. Biol.* **9**, 92–101 (1999).
12. Kramer, B. *et al.* Homogeneous nucleation rates of supercooled water measured in single levitated microdroplets. *J. Chem. Phys.* **111**, 6521–6527 (1999).
13. Bartell, L. S. Nucleation rates in freezing and solid-state transitions. *J. Phys. Chem.* **99**, 1080–1087 (1995).
14. Abraham, F. F. *Homogeneous Nucleation Theory* (Academic, New York, 1974).
15. Steinhart, P. J., Nelson, D. R. & Ronchetti, M. Bond-orientational order in liquids and glasses. *Phys. Rev. B* **28**, 784–805 (1983).
16. Ohmine, I., Tanaka, H. & Wolynes, P. G. Large local energy fluctuation in water. *J. Chem. Phys.* **89**, 5852–5860 (1988).
17. Sasai, M., Ramaswamy, R. & Ohmine, I. Long time fluctuation of liquid water. *J. Chem. Phys.* **96**, 3045–3053 (1992).
18. Walrafen, G. E., Hokmabadi, M. S., Yang, W.-H., Chu, Y. C. & Monosmith, B. Collision-induced Raman scattering from water and aqueous solutions. *J. Phys. Chem.* **93**, 2909–2917 (1989).
19. Saito, S. & Ohmine, I. Translational and orientational dynamics of a water cluster (H_2O)₁₀₈ and liquid water. *J. Chem. Phys.* **102**, 3566–3576 (1995).
20. Metzler, R. & Klafter, J. The random walk's guide to anomalous diffusion: a fractional dynamics approach. *Phys. Rep.* **339**, 1–77 (2000).
21. Weissman, M. B. $1/f$ noise and other slow, non-exponential kinetics in condensed matter. *Rev. Mod. Phys.* **60**, 537–571 (1988).
22. Sasai, M. Instabilities of hydrogen bond network in liquid water. *J. Chem. Phys.* **93**, 7329–7341 (1990).
23. Matsumoto, M. & Ohmine, I. New approach to dynamics of hydrogen bond network in liquid water. *J. Chem. Phys.* **104**, 2705–2712 (1996).
24. Mishima, O. & Stanley, H. E. The relationship between liquid, supercooled and glassy water. *Nature* **396**, 329–335 (1998).
25. Sastry, S., Debenedetti, P. G., Sciortino, F. & Stanley, H. E. Singularity-free interpretation of the thermodynamics of supercooled water. *Phys. Rev. E* **53**, 6144–6154 (1996).
26. Stillinger, F. H. & Weber, T. A. Packing structures and transitions in liquids and solids. *Science* **225**, 983–989 (1984).

Acknowledgements

We thank J. Jortner, and S. Sastry for many stimulating discussions and encouragement. We also thank H. Tanaka, A. Baba and H. Inagaki for cooperative work and valuable discussions. The present study is partially supported by the Grant-in-Aid Scientific Research on Priority Area of 'Condensed Phase Chemical Reaction Dynamics', and by the

Grant-in-Aid for Scientific Research. Calculations were carried out at the Nagoya University Computation Center and the Research Center for Computational Science.

Competing interests statement

The authors declare that they have no competing financial interests.

Correspondence and requests for materials should be addressed to I.O. (e-mail: ohmine@aquacem.nagoya-u.ac.jp).

Active fluidization of polymer networks through molecular motors

D. Humphrey*, C. Duggan*, D. Saha*, D. Smith* & J. Käs*†‡§

* Center for Nonlinear Dynamics, † Institute for Cellular and Molecular Biology, and ‡ Texas Materials Institute, and § Center for Nano and Molecular Science, University of Texas at Austin, Texas 78712, USA

Entangled polymer solutions and melts exhibit elastic, solid-like resistance to quick deformations and a viscous, fluid-like response to slow deformations. This viscoelastic behaviour reflects the dynamics of individual polymer chains driven by brownian motion¹: since individual chains can only move in a snake-like fashion through the mesh of surrounding polymer molecules, their diffusive transport, described by reptation^{2–4}, is so slow that the relaxation of suddenly imposed stress is delayed. Entangled polymer solutions and melts therefore elastically resist deforming motions that occur faster than the stress relaxation time. Here we show that the protein myosin II permits active control over the viscoelastic behaviour of actin filament solutions. We find that when each actin filament in a polymerized actin solution interacts with at least one myosin minifilament, the stress relaxation time of the polymer solution is significantly shortened. We attribute this effect to myosin's action as a 'molecular motor', which allows it to interact with randomly oriented actin filaments and push them through the solution, thus enhancing longitudinal filament motion. By superseding reptation with sliding motion, the molecular motors thus overcome a fundamental principle of complex fluids: that only depolymerization makes an entangled, isotropic polymer solution fluid for quick deformations.

Actin and myosin II are the key elements of the contractile machinery in muscle cells. Myosin's motor domains, or 'heads', bind actin filaments (F-actin) and exploit adenosine triphosphate (ATP) hydrolysis to generate a force to move along polar actin filaments towards the positive end. *In vitro* and in non-muscle cells, myosin II proteins assemble into multimeric bipolar structures with motor domains on both ends^{6–9} known as minifilaments. Several of the myosin heads at the end of these minifilaments attach to actin filaments. When ADP (adenosine diphosphate) is substituted for ATP in solution, the minifilaments crosslink F-actin via the inactive heads. In this case the actin–myosin sample assumes a solid, gelatin-like consistency (Fig. 1a). In the presence of ATP, myosin is active and the sample behaves like a fluid (Fig. 1a). The myosin heads push the actin filaments and collectively induce sliding of filaments in the presence of ATP¹⁰ (Fig. 1b). Similar to two-dimensional motility assays¹¹ in which F-actin moves on myosin heads adsorbed to a cover slide, filaments are unidirectionally pushed by myosin towards their negative ends. The sliding filaments are oriented at a variety of angles with respect to each other.

By inducing active filament sliding instead of thermally driven

filament transport, myosin II has a large effect on the dynamics of actin filaments in networks. Rheological measurements of the frequency-dependent (that is, stress-rate dependent) complex shear modulus, G^* , characterize the effect of these changes in polymer dynamics on actin's viscoelastic properties (Fig. 2). The elastic part of G^* is referred to as the storage modulus G' , while the viscous part is known as the loss modulus G'' . The relation between G' and G'' describes to what extent the polymer sample responds elastically¹². At low frequencies, the polymer solution behaves like a fluid and responds viscously ($G' \leq G''$), whereas at higher frequencies, the sample responds like rubber by resisting elastically

($G' > G''$). Thus, frequency-dependent rheology is ideally suited to distinguish elastic from fluid solutions.

We compared entangled solutions of actin filaments to isotropic actin networks with active or inactive myosin II dispersed in them. An actin monomer concentration of $36 \mu\text{M}$ and myosin concentration of $0.14 \mu\text{M}$ in the experiments resulted in a ratio of myosin proteins to actin filaments of ~ 15 , with 2–16 myosin proteins assembled to small bipolar minifilaments (see light-scattering data in Supplementary Information). The addition of inactive myosin led to an increase in the plateau storage modulus G' of a factor of 6 ± 1.3 (see Fig. 2). Inactive myosin acts as a crosslinker, and this gelation process increases the elastic strength of the sample¹³. The addition of ATP, which induces filament sliding, caused a decrease of G' to $40 \pm 10\%$ of G' for actin solutions without myosin (see Fig. 2). Thus, the elastic strength dropped below the value for a plain entangled actin solution. Moreover, G' approximately equalled G'' , indicating that active myosin renders the network more liquid-like.

The interactions of single chains with surrounding polymers, which underlie the viscoelastic behaviour, can be described by an effective-medium treatment often visualized by a 'tube' arising from the topological constraints of neighbouring polymer chains¹. As these constraints oppose deformations¹⁵, stress is relaxed when filaments have left their original, confining tube (independent of the direction the filament moves with respect to the deforming stress). To allow visualization of the mechanism that enables myosin to modulate the elastic strength of actin networks, rhodamine-phalloidin-labelled actin filaments and myosin were incorporated in networks of unlabelled actin filaments. Fluorescence microscopy could then be used to follow the dynamics of individual actin chains within the network⁴. A direct comparison of single filament motion between a network with active motors and an entangled solution of actin filaments shows large differences in speed and directionality (Fig. 3). In the absence of motors, the filament undergoes random brownian motion confined by the surrounding unlabelled actin

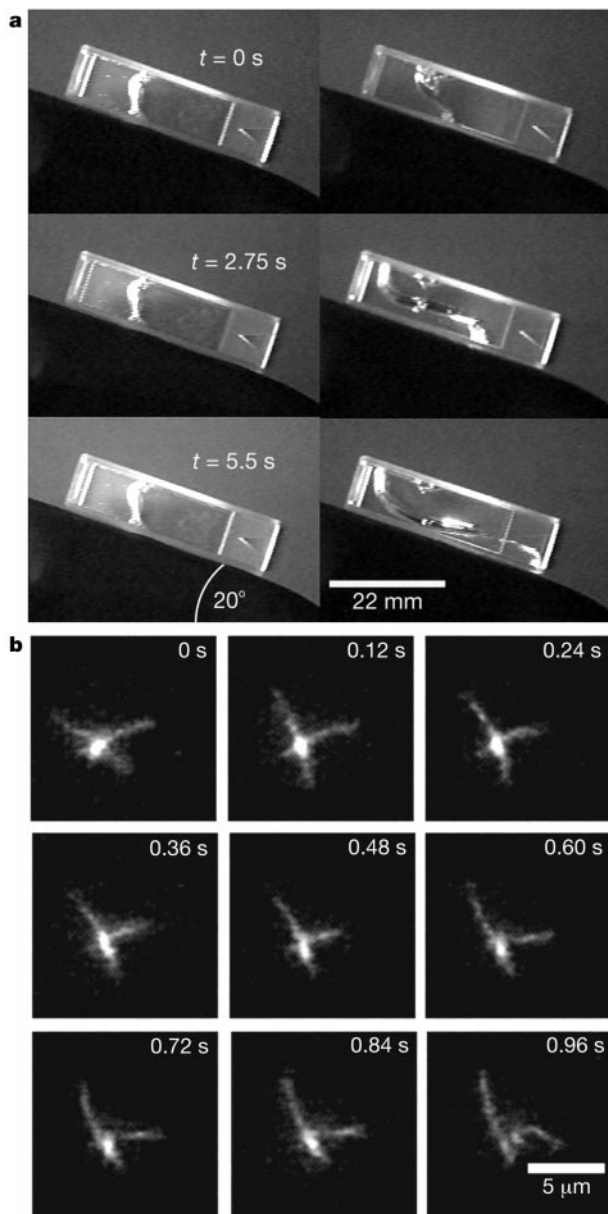


Figure 1 Macroscopic and microscopic influence of bipolar myosin minifilaments on actin networks. **a**, Comparison of the flow properties of actin networks with inactive (left side) or active (right side) myosin dispersed in them. For this purpose a cuvette filled to one-third with sample was tilted from its initial vertical position. With ADP and inactive myosin the samples gelled and behaved like an elastic solid. In the presence of ATP or when caged ATP was released, the active motors caused fluid-like flow properties. **b**, In the presence of ATP, two rhodamine-phalloidin-labelled actin filaments in dilute solution slide along each other while connected by BODIPY FL-labelled myosin (bright spot). The left filament moves to the upper left side with respect to the myosin minifilament and the right filament moves to the right. In the last picture filaments disengage.

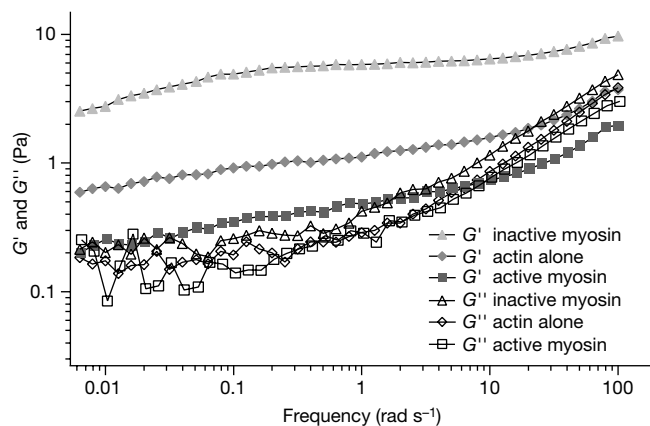


Figure 2 Elastic strength of actin and actin–myosin networks ($36 \mu\text{M}$ actin, $0.14 \mu\text{M}$ myosin, $500 \mu\text{M}$ ATP/ADP). The filled markers display the storage modulus, G' , a measure of the elastic strength. The open markers show the loss modulus, G'' , which characterizes the viscous component. The inactive myosin–actin network shows the highest value of G' . When myosin was activated by ATP the value of G' decreased below the value for the entangled actin solution. Below 0.03 rad s^{-1} G' and G'' are comparable signifying, in effect, a fluid solution. According to our microscopic stress relaxation experiments (see Fig. 4 inset) the onset of liquefaction should occur at 0.1 rad s^{-1} . The slightly lower onset is caused by the polydispersity of the sample. Between 0.03 and 5 rad s^{-1} a small elastic plateau remains for the active actin–myosin network. At higher frequencies ($> 5 \text{ rad s}^{-1}$) the rheometer probes the internal dynamics of filaments indicated by the typical crossover between G' and G'' . In the high-frequency regime the active motors cause a transition from a coil-like to a rod-like behaviour¹⁶ inducing the early onset of the internal dynamics regime.

filaments, with no net transport being detectable on a timescale of ten seconds. The filament remains enclosed in the original tube formed by the surrounding filaments. In actin–myosin networks, myosin induces longitudinal sliding of filaments when ATP is added. At least 98% of the studied filaments in these dense three-dimensional entangled F-actin networks displayed sliding activity when active myosin was present, with an experimentally determined average sliding speed of $1.3 \pm 0.3 \mu\text{m s}^{-1}$. Under ADP conditions, filaments are immobilized owing to crosslinking by inactive myosin (data not shown).

In actin–myosin solutions under ATP conditions, the time for a filament to disengage from its original tube confinement, τ , dras-

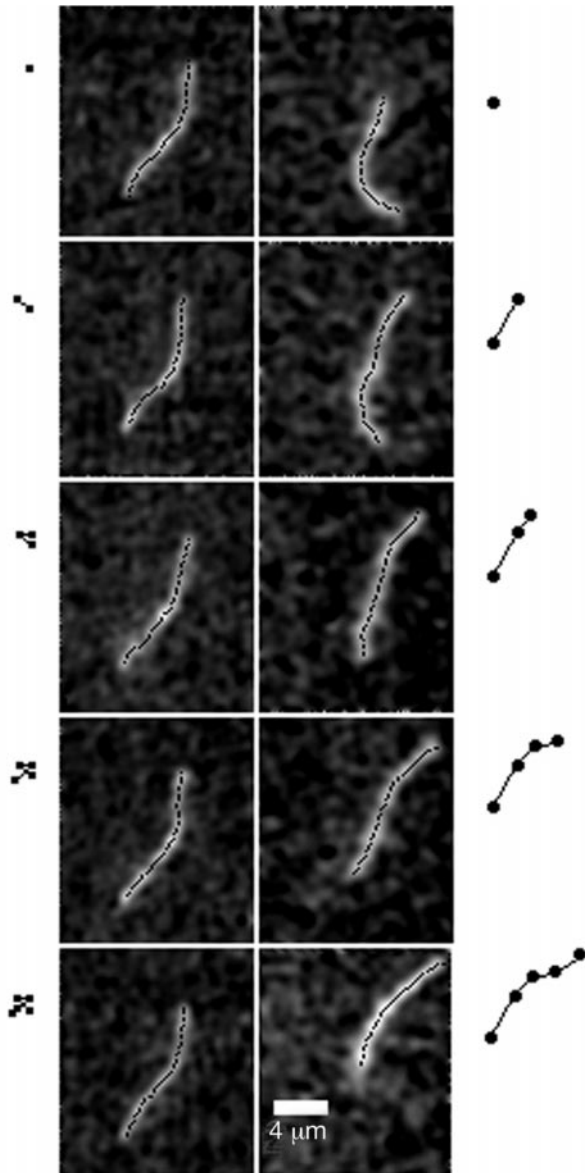


Figure 3 Motion of a single actin filament in an F-actin solution or an actin–myosin network. Fluorescently labelled filaments are embedded in an unlabelled matrix of filaments (left side) or in an unlabelled network of filaments with active myosin minifilaments present (right side). The time interval between successive pictures is 2.5 s. The left filament solely undergoes brownian motion restricted by the surrounding filaments. Within 10 s no net transport of the polymer chain was observed. The right filament shows directional sliding induced by myosin, resulting in a quick transport of the filament. The dashed black lines represent the digital traces of filament contours used to analyse filament motion. The two outer columns depict the motion of the upper filament ends without (squares) and with (circles) myosin.

tically decreases, because filament sliding prevails over random backward and forward motions (Fig. 4 inset). For deformations slower than τ , solutions of actin filaments appear fluid, but for quicker motions an elastic stress opposes the distortion because filaments are confined in their surrounding tubes. This stress is relaxed when a filament leaves its original tube, that is, moves in a random direction over a distance equal to its length. As can be seen in the inset of Fig. 4, the tube disengagement time (that is, local stress relaxation time), τ , depended linearly on the filament length, L , when motors caused filament sliding. In entangled actin solutions the relaxation time depended on the filament length as $\tau \propto L^3$, in agreement with the reptation concept^{2,4}. Thus, in actin networks with a polydisperse filament length distribution ($\sim 1\text{--}130 \mu\text{m}$) and a mean filament length of $10 \mu\text{m}$, the average stress relaxation time significantly decreased from $500 \pm 100 \text{ s}$ for pure actin solutions to $8 \pm 0.4 \text{ s}$ when active myosin was added. Inactive myosin froze filament transport by crosslinking the filaments; no relaxation occurred over an observation time of 20 minutes.

As a result, an actin solution with active myosin will mostly relieve macroscopic stress within $\sim 8 \text{ s}$ and should be fluid-like for all deformations performed at a rate slower than $1/8 \text{ s}^{-1}$, enabling the sample to flow out of a cuvette (see Fig. 1a). Consequently, the rheological behaviour should change to $G' \approx G''$ for shear frequencies below $\sim 0.1 \text{ rad s}^{-1}$. Nevertheless, a remnant indication of elasticity was found even below $\sim 0.1 \text{ rad s}^{-1}$ in networks of actin filaments and active myosin (Fig. 2). Because this decrease in residual elasticity directly correlated with our efforts to purify the myosin from dysfunctional myosin heads without motor activity (also known as dead myosin), we conclude that this minor elastic

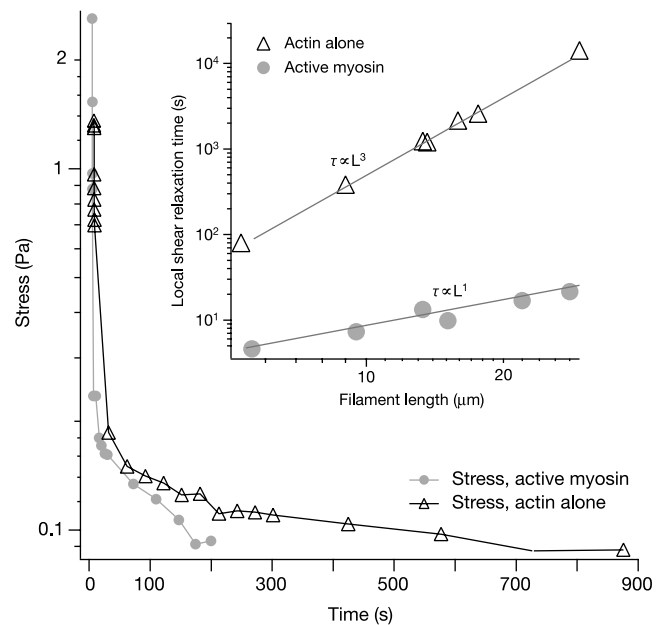


Figure 4 Temporal stress relaxation behaviour in actin and actin–myosin networks. The main plot displays the bulk stress relaxation behaviour in response to a prior 3% step strain. The relaxation of an entangled F-actin solution (triangles) is compared to actin networks with active myosin (filled circles). Stress below 0.1 Pa cannot be reliably detected with our rheometer. The inset shows a logarithmic plot of the time, τ , a filament needs to move a distance equal to its length (that is, the local stress relaxation time) either in a solution of actin filaments (triangles) or in an actin–myosin network under ATP conditions (filled circles) as function of actin filament length, L . Filaments differing in their length by less than $1 \mu\text{m}$ have been combined into one data point. The relative errors in measurements of τ are 19% and 5% for reptating and sliding filaments, respectively. In an entangled solution, $\tau \propto L^3$; this changes to a linear dependence in the presence of active myosin motors. Furthermore, the observed τ decreases by more than an order of magnitude for active myosin.

contribution primarily originated from an unavoidable trace amount of dead myosin crosslinking the filaments (see Supplementary Information). A density of 1 filament pair crosslinked by dead myosin in 100,000 pairs is sufficient to cause the remaining elastic response^{14,15}. In other words, a small number of elastically active strands were mixed with a large number of filaments exhibiting fluid-like behaviour. The myosin-induced fluidification (reduction of relaxation time and elastic strength) shown experimentally here can be modelled by a diffusive directed motion of the polar filaments in their tube owing to increased longitudinal fluctuations along the filament contour, giving rise to a higher effective temperature¹⁶.

The change in the elastic response of active actin–myosin networks with respect to F-actin solutions is reflected in macroscopic stress relaxation experiments, in which a 3% step strain is applied and the time course of the resulting stress is monitored (see Fig. 4). Active myosin-induced filament sliding increased the macroscopic stress relaxation rate compared to an entangled F-actin solution by nearly an order of magnitude. However, a direct comparison between local stress relaxation by filament sliding and macroscopic stress relaxation is hampered by the presence of dead myosin heads and the polydispersity of F-actin. Polydispersity gives rise to different tube disengagement times contributing to the relaxation process. Moreover, some filaments are not pushed by minifilaments, while trace amounts of dead myosin heads act as crosslinks that prevent complete stress dissipation. The residual undissipated stress due to trace amounts of dead myosin is almost below the stress detection limit for the experiments summarized in Fig. 4, but was more pronounced when more dead myosin was contaminating the sample.

The typical ratios of myosin to actin filaments used in our experiments fall within the range typically found in eukaryotic cells ($n = 3.4\text{--}63$; ref. 17). Although a range of accessory proteins that induce crosslinks hinder filament sliding *in vivo*, crosslinking only holds back transiently the sliding filaments¹³. Thus the interplay between filament sliding and crosslinking may be rather complex. As a result, myosin's ability to modulate viscoelasticity may also be relevant to motile eukaryotic cells, given that the fluidization of the actin cytoskeleton is an essential step in cell motility⁵. □

Methods

Protein purification

Actin powder from rabbit skeletal muscle was prepared according to the original method of ref. 18, as modified in ref. 19. Monomeric actin (G-actin) was extracted by the method of ref. 20. Myosin II was purified from rabbit skeletal muscle according to ref. 21. To remove inactive myosin, 6.3 μM G-actin and 5.2 μM myosin were polymerized for two hours at room temperature in F buffer (10 mM Tris–HCl (pH 7.5), 2 mM MgCl₂, 150 mM KCl, 0.2 mM CaCl₂, 0.5 mM ATP). After two hours, 270 μl of 0.25 M ATP were added to a final ATP concentration of 5 mM. The solution was spun at 4 °C at 100,000g for 90 min. The supernatant containing myosin with active molecular motors was transferred, and the concentration determined using the Bradford assay. The presence of full myosin II in the supernatant was established by SDS–PAGE and by light scattering (see Supplementary Information). This protocol is conventionally used to isolate active cleaved myosin heads, but also turned out to be efficient for full myosin. BODIPY-FL (Molecular Probes) was used to label myosin II according to the Molecular Probes protocol. For labelled and unlabelled myosin, motor activity was checked by actin filament sliding (that is, motility assay) as well as by ATPase activity monitored by a luciferase-based assay (see also Supplementary Information).

Polymer dynamics and rheology

The dynamics of individual rhodamine–phalloidin-labelled actin filaments in F-actin or in actin–myosin networks were visualized and analysed by fluorescence microscopy as previously described²². In all experiments, unless otherwise stated, labelled actin filaments were mixed with unlabelled filaments (ratio of 1:4000) in F buffer. All experiments were performed with 0.5 mM ATP or ADP present, and either with or without 140 nM myosin II at a final actin concentration of 36 μM . The unlabelled filaments were polymerized around the fluorescently labelled filaments. A 30 min polymerization time was sufficient for this concentration of actin. Based on an average filament length of 10 μm and on the fact that 14 actin monomers form an actin filament segment of 37 nm length, the ratio of myosin to actin filament n was calculated as $n = (c_{\text{myosin}}N_{\text{fil}})/c_{\text{actin}}$, where c_{actin} is the molar actin concentration, c_{myosin} is the molar myosin concentration, and N_{fil} is the average

number of monomers per filament. Although it was a rare event to find two labelled actin filaments simultaneously connected by a labelled myosin minifilament ($n = 5$, for example, Fig. 1b), good data ($n = 50$, for example, Fig. 3) have been obtained from observing a sliding labelled filament with unlabelled partners. The time a filament needs to move a distance equal to its length in the surrounding actin matrix has been measured as previously described^{12,22} for reptating filaments and determined by direct observation for the sliding filaments.

Rheological measurements were performed with a commercial fluid rheometer (Rheometrics Model 8400) and a newly developed Mooney–Couette torsion pendulum rheometer that had been designed for simultaneous microscopy of actin filaments and measurement of G^* . The rheological data were reproducible for six different actin and myosin preparations; at least three measurements were performed for each condition and protein preparation. To obtain consistent data, it is absolutely necessary to avoid large amounts of dead myosin heads with the precautions described above. Simultaneous rheology and microscopy excluded changes in the actin network structure, such as filament bundling and filament breakage, as the cause of the loss of elasticity in the presence of active myosin. Furthermore, the actin filaments maintained their random orientation in active actin–myosin networks. No myosin-induced ordering of actin filaments—as previously described for microtubules in the presence of molecular motors²³—was observed at the actin and myosin concentrations used. The presence of ATP throughout the experiments was verified by the observation of sliding filaments as well as by luciferase activity.

Received 4 February 2001; accepted 18 February 2002.

- Doi, M. & Edwards, S. F. *The Theory of Polymer Dynamics* (Clarendon, Oxford, 1986).
- de Gennes, P. G. Reptation of a polymer chain in the presence of fixed obstacles. *J. Chem. Phys.* **55**, 572–579 (1971).
- Perkins, T. T., Smith, D. E. & Chu, S. Direct observation of tube-like motion of a single polymer chain. *Science* **264**, 819–822 (1994).
- Käs, J., Strey, H. & Sackmann, E. Direct visualization of reptation for semiflexible actin filaments. *Nature* **368**, 226–229 (1994).
- Taylor, D. L. & Condeelis, J. S. Cytoplasmic structure and contractility in amoeboid cells. *Int. Rev. Cytol.* **56**, 57–144 (1979).
- Reisler, E., Smith, C. & Seegan, G. Myosin minifilaments. *J. Mol. Biol.* **143**, 129–145 (1980).
- Niederman, R. & Pollard, T. D. Human platelet myosin. *J. Cell Biol.* **67**, 72–92 (1975).
- Sinard, J. H. & Pollard, T. D. Acanthamoeba myosin II minifilaments assemble on a millisecond time scale with rate constants greater than those expected for a diffusion limited reaction. *J. Biol. Chem.* **265**, 3654–3660 (1990).
- Verkhovskiy, A. B., Svitkina, T. M. & Borisov, G. G. in *Cell Behaviour: Control and Mechanism of Motility* (eds Lackie, J. M., Dunn, G. A. & Jones, G. E.) 207–222 (Biochem. Soc. Symp. 65, Portland Press, London, 1999).
- Honda, H., Nagashima, H. & Asakura, S. Directional movement of F-actin in vitro. *J. Mol. Biol.* **191**, 131–133 (1986).
- Kron, S. J. & Spudis, J. A. Fluorescent actin filaments move on myosin fixed to a glass surface. *Proc. Natl Acad. Sci. USA* **83**, 6272–6276 (1986).
- Gupta, R. K. *Polymer and Composite Rheology*, 2nd edn (Marcel Dekker, New York, 2000).
- Wachsstock, D. H., Schwarz, W. H. & Pollard, T. D. Cross-linker dynamics determine the mechanical properties of actin gels. *Biophys. J.* **66**, 801–809 (1994).
- Morse, D. C. Viscoelasticity of concentrated isotropic solutions of semiflexible polymers. 2. Linear response. *Macromolecules* **31**, 7044–7067 (1998).
- Isambert, H. & Maggs, A. C. Dynamics and rheology of actin solutions. *Macromolecules* **29**, 1036–1040 (1996).
- Liverpool, T. B., Maggs, A. C. & Ajdari, A. Viscoelasticity of solutions of motile polymers. *Phys. Rev. Lett.* **86**, 4171–4174 (2001).
- Bray, D. *Cell Movements* (Garland, New York, 1992).
- Straub, F. B. Actin II. *Studies Inst. Med. Chem. Univ. Szeged* **3**, 23–27 (1943).
- Adelstein, R. S., Godfrey, J. E. & Kiely, W. W. G-actin: preparation by gel filtration and evidence for double stranded structure. *Biochem. Biophys. Res. Commun.* **12**, 34–38 (1963).
- MacLean-Fletcher, S. D. & Pollard, T. D. Viscometric analysis of the gelation of Acanthamoeba extracts and purification of two gelation factors. *J. Cell Biol.* **85**, 414–428 (1980).
- Margossian, S. S. & Lowey, S. Preparation of myosin and its subfragments from rabbit skeletal muscle. *Methods Enzymol.* **85**, 55–71 (1982).
- Käs, J. *et al.* F-Actin, a model polymer for semiflexible chains in dilute, semidilute, and liquid crystalline solutions. *Biophys. J.* **70**, 609–625 (1996).
- Nedelec, F. J., Surrey, T., Maggs, A. C. & Leibler, S. Self-organization of microtubules and motors. *Nature* **389**, 305–308 (1997).

Supplementary Information accompanies the paper on Nature's website (<http://www.nature.com>).

Acknowledgements

We thank M.E. Cheney for providing a commercial fluid rheometer, and J. Prost for help with the interpretation of the results. We also thank the following for discussions; H. Swinney, C. Moncman, F. Jülicher, A. Maggs, T. Liverpool, D. Morse, J. Guck, D. Martin, P.A. Janmey, F. Brochard, K. Browning and P.G. de Gennes.

Competing interests statement

The authors declare that they have no competing financial interests.

Correspondence and requests for materials should be addressed to J.K. (e-mail: kas@chaos.ph.utexas.edu).